

Renal Ultrasound Using Parametric Imaging Techniques to Detect Changes in Microstructure and Function

MICHAEL F. INSANA, PhD, TIMOTHY J. HALL, PhD, JOHN G. WOOD, PhD, AND ZHONG-YU YAN, MD

Insana MF, Hall TJ, Wood JG, Yan Z-Y. Renal ultrasound using parametric imaging techniques to detect changes in microstructure and function. *Invest Radiol* 1993;28:720-725.

RATIONALE AND OBJECTIVES. Signal processing techniques have been used to generate parametric ultrasound images that describe properties of tissue microstructure.

METHODS. Images of the average scatterer size (D) and integrated backscatter coefficient (IBC) for normal dog kidneys were examined.

RESULTS. With parametric ultrasound the authors identified sources of cortical backscatter and observed microanatomical changes corresponding to ischemia. In particular, scatterer size images acquired *in vitro* and *in vivo* show it is possible to rapidly assess changes and differences in the average glomerular diameter and the average arteriolar cross-sectional diameter.

CONCLUSIONS. A more direct interpretation of sonographic image data is possible with this new type of imaging. Parametric imaging may have a diagnostic role as a means to differentiate among conditions producing increased cortical echogenicity and to detect important structural indicators such as glomerular hypertrophy.

KEY WORDS. Kidney; microstructure; quantitative imaging; ultrasound.

ECHO SIGNALS USED to generate sonograms contain a considerable amount of information about the microscopic structure of soft tissues. The echoes are formed by interactions between tissue structures and sound waves, and depend on the size, number, shape, orientation, and elastic

properties of scattering sites in tissue. Instead of integrating all this information into a single B-mode image, which is currently done, parametric ultrasound methods display tissue parameters individually to allow a more direct interpretation of the data in terms of the microstructure and function of tissue.

In previous laboratory studies, we examined the renal parenchyma of dog kidneys using nonimaging, parametric ultrasound methods.^{1,2} Our goal was to identify the microscopic anatomy that scatters sound and thereby produces the sonographic image. We found that the intensity of sound backscattered from the cortex varied depending on the angle between the ultrasound beam axis and the long axis of the nephron, as Rubin et al observed qualitatively.³ This structural anisotropy produces brighter regions in the cortex when the beam is perpendicular to the predominant nephron orientation, as shown in Figure 1. Using signal processing methods and correlations with histologic observations, we were able to exploit this anisotropic nature and identify principal sources of scattering in the renal cortex. From *in-vitro* measurements, we concluded that glomeruli dominate backscatter properties at frequencies less than 5 MHz and that arterioles and tubules dominate at frequencies greater than 5 MHz.¹ Subsequent *in-vivo* measurements using ischemic and obstructed dog kidneys provided further support of our hypotheses regarding the role of these structures as scatterers and also demonstrated our ability to monitor changes in renal function.²

Based on the nonimaging studies, we concluded that advanced signal processing of ultrasonic signals provides more specific and detailed information than that available with conventional sonographic imaging alone. In particular, parametric ultrasound techniques can be used quantitatively to follow changes in microanatomy concomitant with changes in function. In the kidney, this information is ob-

From the Departments of Diagnostic Radiology, Surgery, and Physiology, University of Kansas Medical Center, Kansas City, Kansas.

Supported by NIH grant DK43007 and the Clinical Radiology Foundation at Kansas University Medical Center.

Reprint requests: Michael F. Insana, PhD, Department of Radiology, KUMC, 3901 Rainbow Blvd., Kansas City, KS 66160-7234

Received November 16, 1992, and accepted for publication, after revision, March 10, 1993.

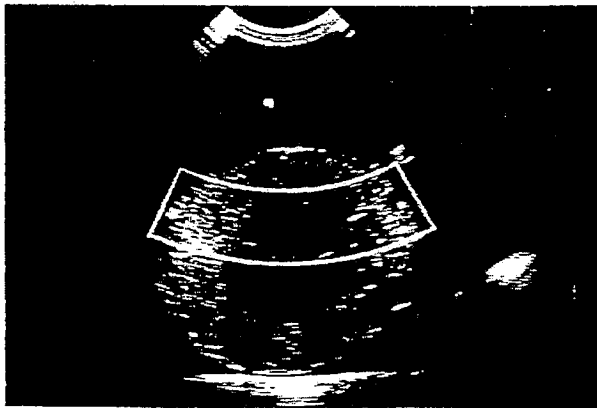


Fig. 1. A B-mode image through a mid-axial plane of an excised dog kidney placed in saline. The analysis region is outlined. Cortical echogenicity is enhanced on both sides of the analysis region where the beam axis is perpendicular to the predominant nephron orientation.

tained with just two parameters: scatterer size (D) and integrated backscatter coefficient (IBC). Low-frequency scatterer size estimates may be particularly important in the kidney, because glomerular hypertrophy has been found to be an early indicator of disease⁴ and is closely correlated with glomerular sclerosis, proteinuria, and progressive renal deterioration.⁵

Many diagnostic applications require greater spatial resolution than the measurements described above provide, where relatively large volumes of tissue (50 to 100 mm³) were used to achieve 10% to 20% parameter uncertainties. We sacrificed spatial resolution in these early studies to attain high-precision estimates in regions homogeneous in these parameters. In this article, we will discuss investigations relative to the question: Can parametric imaging with spatial resolution on the order of conventional imaging improve the information content of diagnostic ultrasound in kidneys?

Materials and Methods

Whole kidneys from male mongrel dogs weighing 20 to 28 kg were imaged. Data were acquired for excised and live perfused kidneys. For the in-vitro studies, freshly excised kidneys were placed in normal saline at 22°C and scanned in a coronal plane 1 cm anterior of center (Fig. 2). Each kidney was stored on ice overnight, and data were recorded approximately 14 hours after excision. For the in-vivo studies, data were recorded while scanning the kidneys of anesthetized dogs, immediately after an unrelated experiment. The left kidney was exposed transabdominally through a midline incision. An aortic clamp positioned proximal to the renal artery was used to control the mean renal perfusion pressure (P_a) to both kidneys. P_a was measured with a pressure transducer introduced through an aortic cannula positioned distal to the aortic clamp and near the renal artery. Further details of the surgical procedure are described elsewhere.²

Sound waves traveled to the kidney through a block of low-

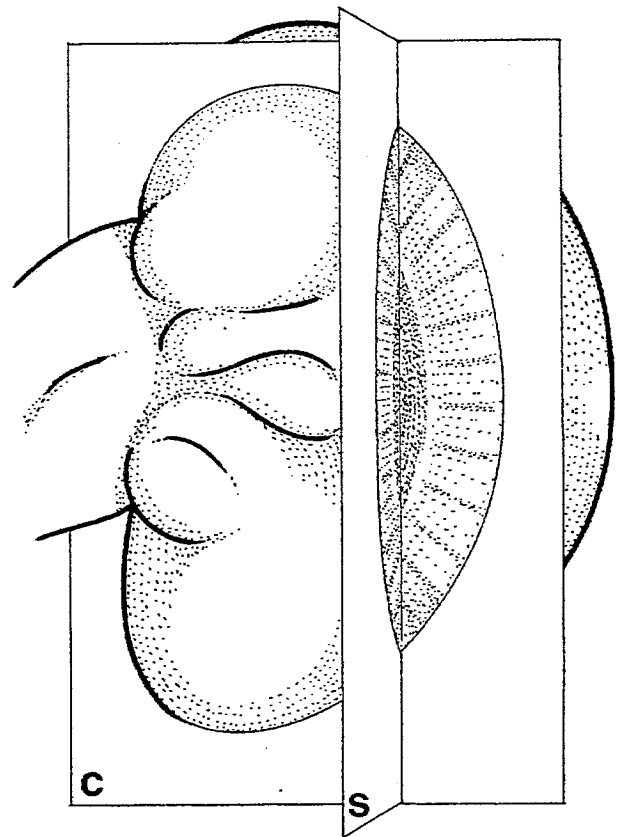


Fig. 2. A cutaway view of the dog kidney. In vitro images, shown in Figures 3 and 4, were obtained in a coronal plane (c). In vivo images, shown in Figure 5, were obtained in a sagittal plane (s).

scattering, graphite-gel material with otherwise tissue-like acoustic properties ($c = 1,540$ m/s, $\alpha = 0.4$ dB/cm/MHz, $\rho = 1.03$ g/cm³). The stand-off material was molded to the shape of the organ and coupled to the transducer and kidney using a water-soluble gel. The advantages of this material over a saline path are that it maintains the center of the analysis region at the focal length and closely approximates the ultrasonic attenuation of renal cortex. Uniform attenuation over the beam path eliminates ultrasonic "beam-hardening" effects (see Discussion section). Images were obtained in-vivo in a sagittal plane approximately 1 cm lateral of center (Fig. 2).

We have previously described the signal processing methods used for parameter estimation and image formation.⁶ The following summarizes the basic procedures and also provides important experimental details.

Unprocessed, radio-frequency echo signals were acquired directly from a mechanical sector scanhead and real-time imaging system (ATL Model 600C, Advanced Technology Laboratories, Inc. Bothell, WA). The peak frequency and -20 dB bandwidth of the transducer was 7.0 MHz, the diameter was 6 mm, and the focal length was 45 mm. An electronic gate was built and used to select tissue regions for analysis by viewing a real-time display and then digitally recording the radio-frequency echo signals corresponding to that region (Fig. 1). Analysis regions were centered about the focal length. Echo signals were low pass filtered (<11 MHz) and

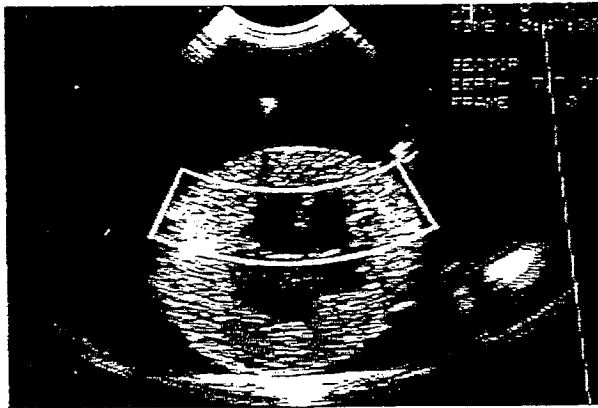


Fig. 1. A B-mode image through a mid-axial plane of an excised dog kidney placed in saline. The analysis region is outlined. Cortical echogenicity is enhanced on both sides of the analysis region where the beam axis is perpendicular to the predominant nephron orientation.

tained with just two parameters: scatterer size (D) and integrated backscatter coefficient (IBC). Low-frequency scatterer size estimates may be particularly important in the kidney, because glomerular hypertrophy has been found to be an early indicator of disease⁴ and is closely correlated with glomerular sclerosis, proteinuria, and progressive renal deterioration.⁵

Many diagnostic applications require greater spatial resolution than the measurements described above provide, where relatively large volumes of tissue (50 to 100 mm³) were used to achieve 10% to 20% parameter uncertainties. We sacrificed spatial resolution in these early studies to attain high-precision estimates in regions homogeneous in these parameters. In this article, we will discuss investigations relative to the question: Can parametric imaging with spatial resolution on the order of conventional imaging improve the information content of diagnostic ultrasound in kidneys?

Materials and Methods

Whole kidneys from male mongrel dogs weighing 20 to 28 kg were imaged. Data were acquired for excised and live perfused kidneys. For the in-vitro studies, freshly excised kidneys were placed in normal saline at 22°C and scanned in a coronal plane 1 cm anterior of center (Fig. 2). Each kidney was stored on ice overnight, and data were recorded approximately 14 hours after excision. For the in-vivo studies, data were recorded while scanning the kidneys of anesthetized dogs, immediately after an unrelated experiment. The left kidney was exposed transabdominally through a midline incision. An aortic clamp positioned proximal to the renal artery was used to control the mean renal perfusion pressure (P_a) to both kidneys. P_a was measured with a pressure transducer introduced through an aortic cannula positioned distal to the aortic clamp and near the renal artery. Further details of the surgical procedure are described elsewhere.²

Sound waves traveled to the kidney through a block of low-

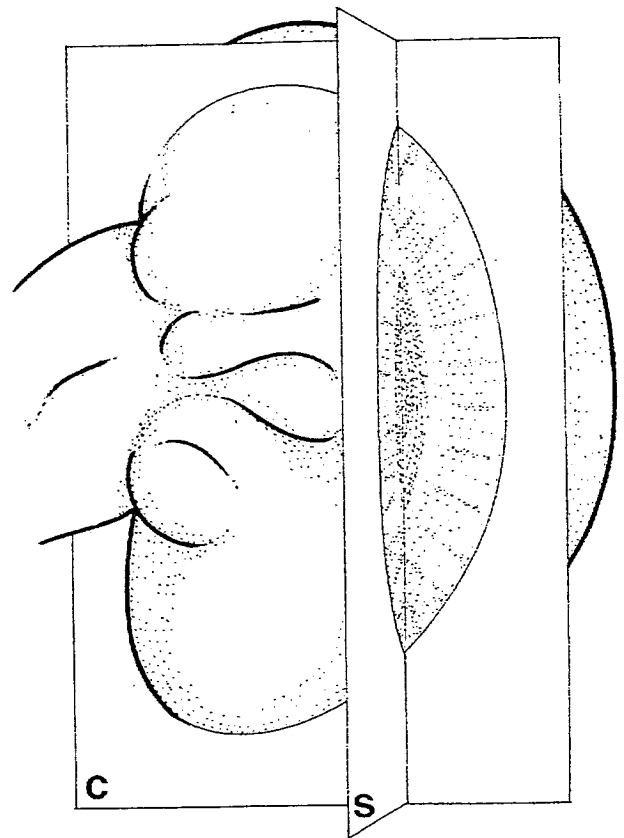


Fig. 2. A cutaway view of the dog kidney. In vitro images, shown in Figures 3 and 4, were obtained in a coronal plane (c). In vivo images, shown in Figure 5, were obtained in a sagittal plane (s).

scattering, graphite-gel material with otherwise tissue-like acoustic properties ($c = 1,540$ m/s, $\alpha = 0.4$ dB/cm/MHz, $\rho = 1.03$ g/cm³). The stand-off material was molded to the shape of the organ and coupled to the transducer and kidney using a water-soluble gel. The advantages of this material over a saline path are that it maintains the center of the analysis region at the focal length and closely approximates the ultrasonic attenuation of renal cortex. Uniform attenuation over the beam path eliminates ultrasonic "beam-hardening" effects (see Discussion section). Images were obtained in-vivo in a sagittal plane approximately 1 cm lateral of center (Fig. 2).

We have previously described the signal processing methods used for parameter estimation and image formation.⁶ The following summarizes the basic procedures and also provides important experimental details.

Unprocessed, radio-frequency echo signals were acquired directly from a mechanical sector scanhead and real-time imaging system (ATL Model 600C, Advanced Technology Laboratories, Inc. Bothell, WA). The peak frequency and -20 dB bandwidth of the transducer was 7.0 MHz, the diameter was 6 mm, and the focal length was 45 mm. An electronic gate was built and used to select tissue regions for analysis by viewing a real-time display and then digitally recording the radio-frequency echo signals corresponding to that region (Fig. 1). Analysis regions were centered about the focal length. Echo signals were low pass filtered (<11 MHz) and

digitally recorded at 50 megasamples per second under computer control. All signal processing and image display occurred off-line on a workstation.

Seventy-five scan lines were recorded in each scan plane, where each scan line was 15 μ s in duration (\approx 11.6-mm slice thickness). Acoustic parameters were estimated for each waveform, such that each transducer revolution generated data for one horizontal row of pixels in a parametric image. The scanhead was mounted on a linear translation device and moved in elevation, i.e., perpendicular to the scan plane, before recording data from another revolution of the transducer. One hundred twenty-eight scan planes used to generate the vertical axis in parametric images; the image format was 75 \times 128 pixels, and the pixel dimensions were 0.5 \times 0.5 mm. This two-dimensional C-scan method for acquiring data offered the greatest possible spatial resolution for parametric imaging. Because the transducer element was circularly symmetric, the parametric image resolution in the horizontal and vertical directions were equal and were determined by the lateral beam properties within the focal range. C-scan slice thickness could be reduced by range-gating the recorded waveforms.

Two acoustic parameters, D and IBC, and one statistical parameter, χ^2 , were determined from the backscatter coefficient (BSC) measured as a function of ultrasonic frequency over the bandwidth of the transducer.⁶ First, we estimate the average scatterer size (D) by studying the frequency dependence of the backscatter coefficient. The procedure is designed to compare BSC measurements from tissue with a look-up table of BSC values predicted for the frequency bandwidth of the measurement. Predicted values are computed from scattering theory based on prior knowledge of tissue morphology and the geometry of the experiment, e.g., focal length and aperture.⁷ For kidney cortex, the set of functions stored in the look-up table is generated assuming a range of possible scatterer sizes between 10 and 300 μ m in 1 μ m increments. The size estimate is the value of D corresponding to the computed function that yields the minimum chi-squared (χ^2) value⁸ when fit to the data.

Second, χ^2 estimates were used to form χ^2 images to show how well measured BSC values were predicted throughout the analysis region. Pixels displaying large χ^2 values indicate that the predicted BSC values poorly represent the actual backscatter properties for

that region. The χ^2 image is a statistical indication of the accuracy of D estimates.⁶ We use χ^2 images to help discriminate between regions of varying tissue structure and those where the scattering model used to predict BSC values is inappropriate. For fixed sampling rates, longer waveform segments provide more uncorrelated spectral points within the bandwidth, and therefore lower χ^2 values and more precise D estimates, i.e., lower parametric image noise. However, long waveform segments also mean large image slice thicknesses and the possibility of significant partial volume effects in heterogeneous tissues. We found that 10 μ s waveform segments (7.7-mm slice thickness) provided a reasonable trade-off between image noise and partial volume effects for kidneys.

Third, we estimated the integrated backscatter coefficient (IBC). For kidneys, the transition frequency between backscatter dominated by large and small scatterers is 5 MHz; thus, D estimates were obtained by analyzing the frequency dependence of BSC within the transducer bandwidth above and below this value. We also averaged BSC values, often over the same frequency ranges, to obtain IBC estimates.⁶ Whereas the average scatterer size controls how BSC varies with frequency, the number density, average impedance, and size of scatterers determine IBC. Theoretically, IBC images could provide greater resolving power than today's sonograms, because the effects of attenuation and the pulse-echo point-spread function have been accounted for in the analysis. Inhomogeneities in overlying tissues produce wavefront distortions that reduce our ability to eliminate these effects reproducibly.

Results

Parametric images of D , IBC, and χ^2 were formed, along with amplitude (B-mode) images, from each data set. Coronal view images of an excised dog kidney are shown in Figure 3. All four images were computed from one C-scan data set. The radio-frequency echo signals were filtered to include frequencies between 2.0 MHz and 5.0 MHz for the D and χ^2 images. Full bandwidth (2.0–9.0 MHz) was used to generate the B-mode and IBC images.

Characteristic of the B-mode image on the left is the



Fig. 3. B-mode and parametric images of an excised dog kidney. Arrow indicates the location of the renal artery.

highly echogenic pelvis, echolucent medulla, and moderately echogenic cortex. The IBC image appears similar to the B-mode image, except that some structures are better defined. For example, the renal artery is more clearly visible entering the pelvis in the IBC image (arrow in Fig. 3). Also, the radial lines of the cortex, obvious by direct visual inspection of the organ tissue,¹ are barely visible in the IBC image, but are not visible in the B-scan image. We averaged pixel values in the scatterer size image to find $D = 190 \pm 34 \mu\text{m}$ in the cortex. This value is in agreement with our previous in-vitro measurement of $220 \pm 15 \mu\text{m}$ using nonimaging techniques.¹ The earlier D measurements were made by averaging 20 echo spectra each computed from 10 μs waveform segments, and D was determined from an average of four different kidneys. The present D estimates are obtained from a scatterer size image of one kidney. In this case, D is measured for each 10 μs waveform segment. Those D values are the pixels in the size image, which when averaged give the mean value of $190 \mu\text{m}$ for the cortex. The uncertainty in the mean scatterer size pixel value is approximately twice that obtained by the nonimaging technique.

The χ^2 image shows that the scattering model used to estimate D yields a similar fit to the backscatter data throughout the kidney, except in the medulla.⁶ The large χ^2 values in the medulla are consistent with the very low signal amplitude resulting from weak backscatter and reflect the large electronic noise component in those signals.

Two scatterer size images are shown in Figure 4 using the same in-vitro data set for images in Figure 3 but over different, nonoverlapping frequency bands as indicated. At low frequencies (left), $D = 190 \pm 34 \mu\text{m}$ in the cortex, which corresponds to the histologically measured estimates of glomerular diameter. Cortico-medullary contrast is marked and in accordance with the absence of glomeruli in the medulla. At high frequencies (right), $D = 75 \pm 25 \mu\text{m}$ in the cortex, which corresponds to the cross-sectional di-

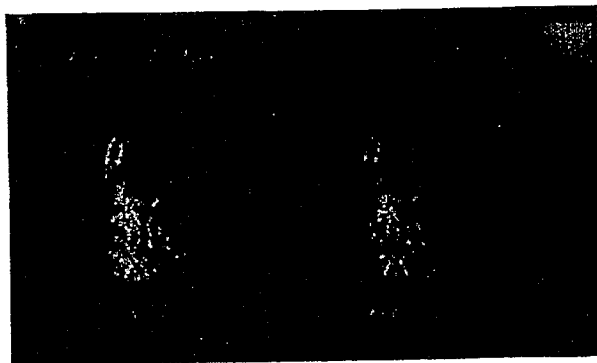


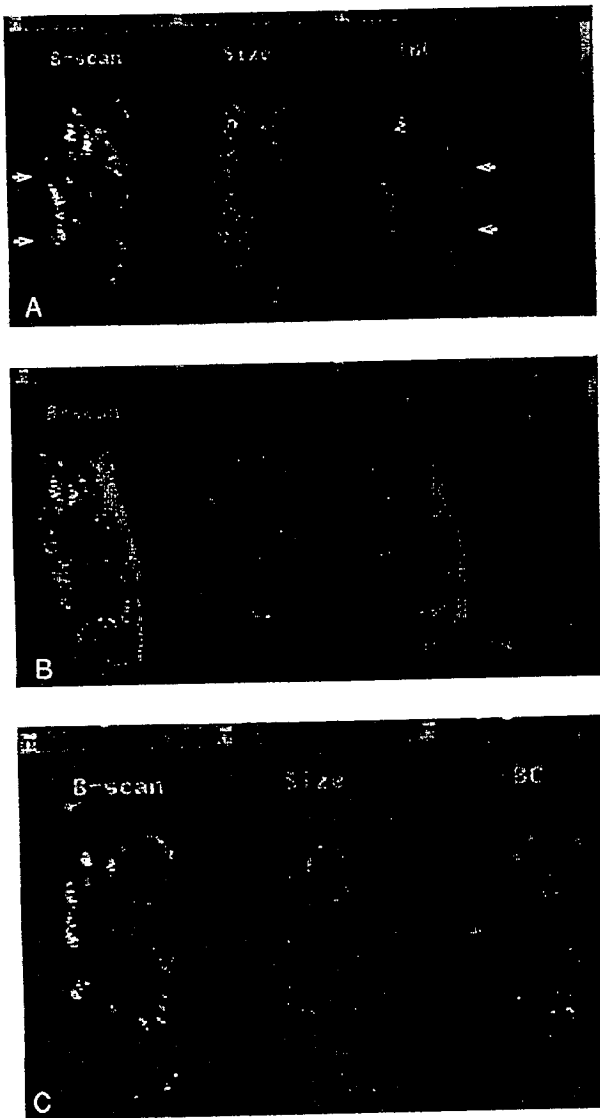
Fig. 4. Scatterer size (D) images for different frequency ranges for an excised dog kidney. Contrast between the cortex and medulla varies with frequency as the relative backscatter from different size structures changes.

ameters of arteriole and tubule elements. (Note that the two images in Fig. 4 are scaled independently.) Cortico-medullary contrast is greatly reduced for high frequencies, because the principal scattering structures—tubules and arterioles—are similar in both tissue types. We conclude from Figure 4 that different structures can be emphasized in scatterer size images by adjusting ultrasonic frequency. Large fat globules in the pelvis produce bright pixel values in all the images of Figure 3, except the χ^2 image. The appearance of the χ^2 image indicates that the scattering models used to estimate D apply equally well to most regions of the kidney. The exception is the very weakly scattering medulla, where the electronic noise in the echo signal is large.

B-mode and parametric images acquired in vivo and at high frequencies ($> 5 \text{ MHz}$) are shown in Figure 5. The top row of images were obtained from normally perfused kidneys, i.e., $P_a = 125 \text{ mm Hg}$. The middle row of images were obtained during a 10-minute ischemic period, where $P_a = 35 \text{ mm Hg}$. The bottom row of images were obtained once P_a was restored to its pre-ischemic value. (Some pixel rows are displaced horizontally in Fig. 5 because of tissue movement during respiration.)

During ischemia, the overall size of the kidney and thickness of the cortex was reduced, and the B-mode, D , and IBC images became brighter. The increase in image brightness is consistent with our previous in-vivo results using nonimaging techniques.² Averaging the results for six dogs, our previous nonimaging measurements revealed a scatterer size increase of $54 \pm 12\%$ and an IBC increase of $113 \pm 38\%$ during ischemia as compared with measurements from normally perfused kidneys.² Averaging pixel values in the cortex, we find from the scatterer size images in Figure 5 that $D = 65 \pm 28 \mu\text{m}$ before ischemia, $D = 79 \pm 30 \mu\text{m}$ during ischemia, and $D = 60 \pm 25 \mu\text{m}$ after ischemia. The 22% increase in scatterer size measured during ischemia was uniformly distributed throughout the cortex, is within the range of a 16% to 89% increase found using nonimaging techniques² and is close to the 32% increase in afferent arteriole diameter measured by Morkrid et al using microspheres.⁹ These data support our hypothesis that at more than 5 MHz, the average cross-sectional diameter of afferent arterioles determines the scatterer size.

Pixel values increased 80% in the cortex of the IBC image during ischemia. That value is comparable to the 113% increase in IBC measured by nonimaging methods.² Increased cortical IBC follows a similar increase in B-mode echogenicity. The clinical literature provides little information on acute sonographic changes in the ischemic kidney. There are reports of increases in cortical echogenicity and cortical thinning after segmental renal infarction in the human.^{10,11} Spies et al¹² provide the most detailed studies of renal infarction. They found no sonographic changes in dog kidneys immediately following segmental artery occlusion. Eight to 24 hours later they observed hypoechoic lesions



Figs. 5A–5C. B-mode and parametric images of a dog kidney scanned in vivo for three different time periods. (A) The cortex (outer echogenic region) and medulla (inner echolucent region) before the ischemic period. (B) Acquired during a period of ischemia. (C) The appearance of the kidney immediately after a 10-minute ischemic period.

forming and remaining until day 7. From 7 to 17 days after infarction, the lesion gradually increased in echogenicity, becoming hyperechoic. The hypoechoic period corresponded to a period of inflammation, while the hyperechoic period corresponded to a contraction and scarring of the infarcted tissues. Our measurements, however, focus on the immediate physiological response of the tissue to ischemia. At present, no known literature provides information for a direct comparison between the data reported in this study and clinical observations.

Discussion

The scatterer size images obtained in vitro and displayed in Figure 4 show that the accuracy and precision of the parameter estimates are sufficient to describe the spatial distribution of D in tissue. Mean values obtained by imaging methods are within the range of those obtained by more precise, nonimaging methods, although the standard error of the mean estimate more than doubled. Therefore, it is possible to separately image different size structures that are spatially mixed, as in the cortex, by varying the ultrasonic frequency.

With the addition of attenuating stand-off material, images obtained in vivo (Fig. 5) show that the cortex is uniform in scatterer size. However, a saline transmission path was used in vitro (Figs. 3 and 4), so that sound traveled a greater distance in tissue near the center because of the kidney's shape (Fig. 1). The greater net attenuation near the center is equivalent to applying a spatially-varying low-pass filter to the echo signals, thereby modifying the frequency dependence of BSC estimates. Consequently, high-frequency BSC values are somewhat lower than average near the center of the kidney, increasing D estimates, and are higher than average near the periphery, decreasing D estimates. For that reason, the in-vitro scatterer size images in Figure 4 appear less uniform (darker near the periphery) than those obtained in vivo (Fig. 5).

Using the stand-off material has at least one disadvantage. The greater overall attenuation further reduced the weak echo-signal amplitude from the medulla so that, at high frequencies, the apparent cortico-medullary contrast for the in-vivo images (Fig. 5) was much higher than for the in-vitro image (Fig. 4, right). The medulla appears dark in Figure 5, because the echo signal is too weak to accurately estimate acoustic parameters and because the image pixels were set to zero. The χ^2 images obtained in vitro, Figure 3, were a warning that the signal-to-noise ratio for medullary echoes was already low, and with the added attenuation in vivo, we can expect poor measurement accuracy in the medulla under clinical conditions.

The in-vivo B-mode and IBC images in Figure 5 display bright horizontal bands across the central one third of the image (see the cortical region between the arrows in Fig. 5A) that do not appear in the scatterer size images. The increased brightness corresponds to a region where the majority of nephrons are aligned perpendicular to the beam axis and, therefore, is a consequence of structural anisotropy. Previously, we conjectured that only those tubular structures aligned nearly perpendicular to the beam axis contribute significantly to backscatter.¹ When the beam and nephron axes are perpendicular, the number density of scattering structures increases, causing an increase in IBC and B-mode image brightness. Because scattering from tubular structures at oblique incidence is small, scatterer size im-

Discussion

The purpose of this study was to determine the relationship between the backscatter coefficient and the structural parameters of the kidney. The backscatter coefficient was measured using a commercial ultrasound system. The structural parameters were measured using a histological method. The results show that the backscatter coefficient is related to the structural parameters of the kidney.

The backscatter coefficient is a measure of the intensity of the backscattered sound. It is related to the structural parameters of the kidney, such as the number density of scatterers and the size of the scatterers. The results of this study show that the backscatter coefficient is related to the structural parameters of the kidney.

The backscatter coefficient is a measure of the intensity of the backscattered sound. It is related to the structural parameters of the kidney, such as the number density of scatterers and the size of the scatterers. The results of this study show that the backscatter coefficient is related to the structural parameters of the kidney.

The backscatter coefficient is a measure of the intensity of the backscattered sound. It is related to the structural parameters of the kidney, such as the number density of scatterers and the size of the scatterers. The results of this study show that the backscatter coefficient is related to the structural parameters of the kidney.

The backscatter coefficient is a measure of the intensity of the backscattered sound. It is related to the structural parameters of the kidney, such as the number density of scatterers and the size of the scatterers. The results of this study show that the backscatter coefficient is related to the structural parameters of the kidney.

n risk, to better understand disease follow the progress of disease and

References

Fishback JL. Identifying acoustic scattering al parenchyma from the anisotropy in acoustic d Med Biol 1991;17:613-626.

Iall TJ. Identifying acoustic scattering sources chyma in vivo by varying arterial and ureteral l Med Biol 1992;18:587-599.

Meyer CR. Anisotropic ultrasonic backscatter ltrasound Med Biol 1988;14:507-511.

Berry PL, et al. Glomerular hypertrophy in ase predicts subsequent progression to focal Kidney Int 1990;38:115-123.

DeFronzo RA. Hyperfiltration and diabetic : beginning? or is it the end? Semin Nephrol

rametric ultrasound imaging from backscatter ents: image formation and interpretation. Ul- 0;12:245-267.

l. Acoustic scattering theory applied to soft e KK Shung, GA Thieme, eds., Ultrasonic al tissues, Boca Raton: CRC Press, 1993:

duction and error analysis for the physical NY: McGraw-Hill; 1969:187-189.

Willassen Y. Diameter of afferent arterioles estimated from microsphere data in the dog 8;42:181-191.

.. Walter JF, Sommer FG. Renal infarction genic mass. AJR 1982;138:759-761.

KJW. Gray scale nephrosonography: current 17:2-6.

ommer TM, et al. Sonographic evaluation of renal arterial occlusion in dogs. AJR 1984;142:

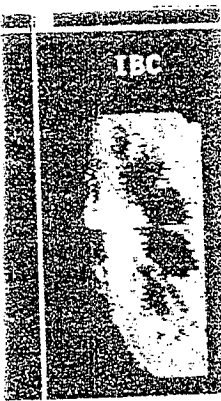


Figure 5. Backscatter and IBC images. The images show the backscatter coefficient (BC) and the integrated backscatter coefficient (IBC) for a kidney. The IBC image shows a bright horizontal band across the central part of the kidney, indicating a region of high backscatter.